Supplementary Information Appendix for:

Visualizing molecular weights differences in supramolecular polymers

Qingyun Li[a], Hanwei Zhang[a], Kai Lou[a], Yabi Yang[a], Xiaofan Ji[a,*], Jintao Zhu[a,*], and Jonathan L. Sessler[b,*]

*Corresponding authors: Xiaofan Ji, Jintao Zhu, and Jonathan L. Sessler
Email: xiaofanji@hust.edu.cn, jtzhu@mail.hust.edu.cn, sessler@cm.utexas.edu

This SI file Consists of:

Other supplementary materials for this manuscript include the following:

Movies S1 and S2

Experimental section

Materials and instruments. All solvents and reagents were of the highest available grade available commercially and used without any further purification unless noted otherwise. Compound **1a** was purchased commercially. Compounds **1**–**3** were synthesized according to literature procedures (1, 2). ^{1}H NMR and ^{13}C NMR spectral studies were performed using either a Bruker Advance 400 or a Bruker Advance 500 MHz spectrometer. High-resolution electrospray ionization mass spectra (ESI-MS) were recorded using a Bruker microOTOF II. The melting points of synthetic compounds were collected on an Inesa WRS-1C device. The UV-vis absorption spectra were collected on a Shimadzu UV-2550 absorption spectrophotometer. Fluorescent emission spectra were recorded on a PerkinElmer LS55 fluorescence spectrophotometer. Viscometry data were measured using a Ubbelohde capillary viscometer immersed in a water bath at 25.0 °C. The inner diameter of the capillary was 0.710 mm.

Scanning electron microscope (SEM). All SEM test samples were prepared by spin coating the solution (10.0 μL) onto a silicon wafer substrate (size: 1.00 × 1.00 cm). Spin coating conditions:

3000 r/m, 120 seconds. The scanning electron microscopy (SEM) samples prepared in this way were tested on a Hitachi SU8010 instrument.

Atomic force microscope (AFM). All AFM test samples were prepared by dripping the solution onto a mica sheet substrate and then subjecting the coated solution to freeze-drying. Atomic force microscope (AFM) images were then captured on a Shimadzu SPM-9700 instrument.

Laser scanning confocal microscopy (LSCM). All test solutions (each 150 μL) were transferred to glass-bottomed cell culture dishes (ϕ15.0 mm) at room temperature. Laser scanning confocal microscopic (LSCM) images were captured using an Olympus FV1200 setup using the highest energy available excitation wavelength (405 nm). The resulting outputs (the LSCM images) were obtained as digital false-color images (3), which were color-coded using the chromaticity of each sample under 405 nm irradiation as observed in the fluorescence spectrum. The fluorescence colors of LSCM images were generated using the fluorescence colors of **M1** + $Zn(OTf)_2$ solutions or **M1** solutions alone photographed under a 365 nm handheld UV lamp. The test samples of LSCM were made up in the same way as those used to take the photographs.

Preparation of M1 + $Zn(OTf)_2$ solutions. Monomer **M1** (29.6 mg, 0.0248 mmol) was dissolved in 1.25 mL chloroform. $Zn(OTf)_2$ (8.80 mg, 0.0242 mmol) dissolved in 1.25 mL methanol was then added to the solution, and the mixture was stirred at room temperature for 1 h. This mixture solution was divided so as to have 50.0 μL in various individual test tubes. After slow evaporation of the organic solvents at 298 K, the solid in each tube was dissolved in 500 μL DMF/H_2O (1/4, v/v) to obtain a stock solution of **M1** + $Zn(OTf)_2$ (2.00 mM total concentration, 500 μL) in each tube. A series of **M1** + $Zn(OTf)_2$ solutions equimolar in each monomer (0.0800 – 1.80 mM total concentration) were prepared by diluting the **M1** + $Zn(OTf)_2$ stock solutions (2.00 mM) with DMF/H_2O (1/4, v/v).

Preparation of M1 solutions. Monomer **M1** (29.6 mg, 0.0248 mmol) was dissolved in 1.25 mL chloroform and 1.25 mL methanol was then added. The mixture solution was divided so as to have 50.0 μL in various individual test tubes. After evaporation of the organic solvents, the solid in each tube was dissolved in 500 μL DMF/H_2O (1/4, v/v) to obtain stock solutions of **M1** (1.00 mM, 500 μL). A series of **M1** solutions (0.0400 – 0.900 mM) were prepared by diluting the **M1** stock solutions (1.00 mM) with DMF/H_2O (1/4, v/v).

Synthesis section

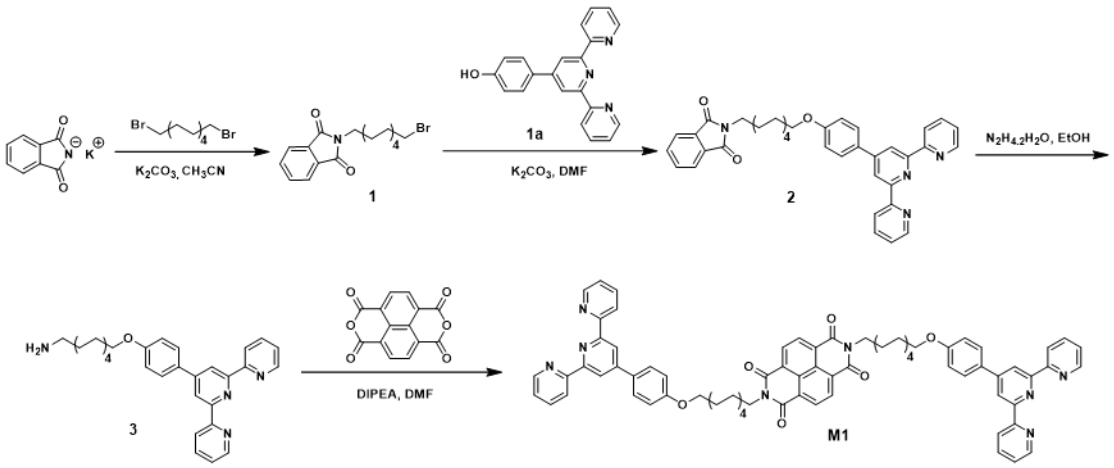

Fig. S1. Synthetic route to monomer **M1**.

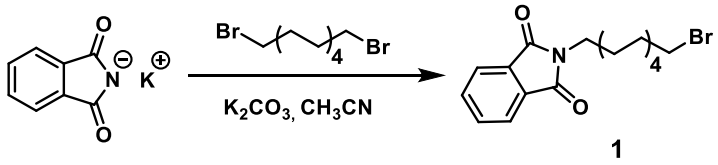

Phthalimide potassium salt (2.10 g, 11.3 mmol) and K_2CO_3 (4.60 g, 33.3 mmol,) were dissolved in CH_3CN (40.0 mL), after which 1,10-dibromodecane (9.80 g, 32.7 mmol) was added to the solution. The mixture was then heated at reflux for 12 hours. The resulting mixture was filtered and the volatiles removed using a rotary evaporator. The crude product was purified by column chromatography (silica gel, petroleum ether/ethyl acetate = 6 : 1) to produce **1** as a white solid (3.80 g, 92.0%). Mp: 58.3 – 59.0 °C. ^{1}H NMR (400 MHz, $CDCl_3$) δ 7.83 – 7.81 (m, 2H), 7.70 – 7.68 (m, 2H), 3.65 (t, 2H, *J* = 7.4 Hz), 3.37 (t, 2H, *J* = 6.9 Hz), 1.85 – 1.78 (m, 2H), 1.68 – 1.61 (m, 2H), 1.40 – 1.35 (m, 2H), 1.30 – 1.26 (m, 10H). ^{13}C NMR (100 MHz, $CDCl_3$) δ 168.5, 133.9, 132.3, 123.2, 38.1, 34.1, 32.9, 29.4, 29.4, 29.2, 28.8, 28.7, 28.2, 26.9. HRMS (ESI$^+$) Calcd for $C_{18}H_{25}BrNO_2$ $[M+H]^+$: 366.1069, found: 366.1063, error –1.6 ppm.

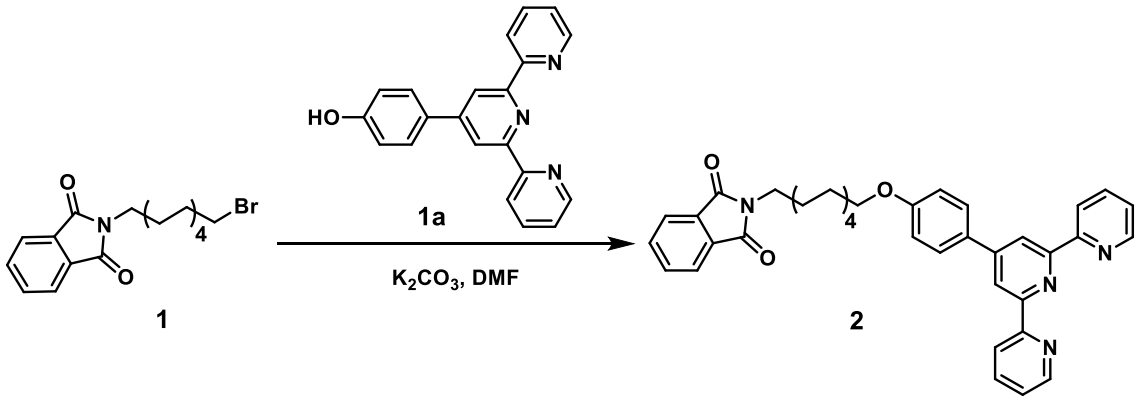

Compound **1a** (1.50 g, 4.62 mmol) and K_2CO_3 (0.950 g, 6.88 mmol) were dissolved in DMF (10.0 mL) and then the solution was stirred at 25.0 °C for 30.0 minutes, after which the bromo-alkylating reagent **1** (2.50 g, 6.85 mmol) was added to the solution. The mixture was heated to 80 °C for 12 h under N_2. Then, the mixture was filtered and the filtrate was concentrated under reduced pressure to give a light yellow residue, which was subsequently recrystallized from $CHCl_3$/hexanes (3x) to give the alkylated product **2** (1.80 g, 63.8%). Mp: 136.4 – 138.1 °C. ^{1}H NMR (400 MHz, $CDCl_3$) δ

8.73 (d, 2H, *J* = 4.0 Hz), 8.70 (s, 2H), 8.67 (d, 2H, *J* = 7.9 Hz), 7.89 – 7.82 (m, 6H), 7.70 – 7.68 (m, 2H), 7.34 (ddd, 2H, *J* = 7.4, 4.8, 1.0 Hz), 7.01 (d, 2H, *J* = 8.8 Hz), 4.02 (t, 2H, *J* = 6.5 Hz), 3.68 (t, 2H, *J* = 7.4 Hz), 1.84 – 1.77 (m, 2H), 1.70 – 1.61 (m, 2H), 1.49 – 1.44 (m, 2H), 1.34 – 1.33 (m, 10H). ^{13}C NMR (100 MHz, $CDCl_3$) δ 168.6, 160.3, 156.6, 156.0, 150.0, 149.3, 137.0, 134.0, 132.3, 130.6, 128.6, 123.9, 123.3, 121.5, 118.4, 115.0, 68.2, 38.2, 29.6, 29.5, 29.5, 29.4, 29.3, 28.7, 27.0, 26.2. HRMS (ESI$^+$) Calcd for $C_{39}H_{39}N_4O_3$ $[M+H]^+$: 611.3022, found: 611.3021, error –0.16 ppm.

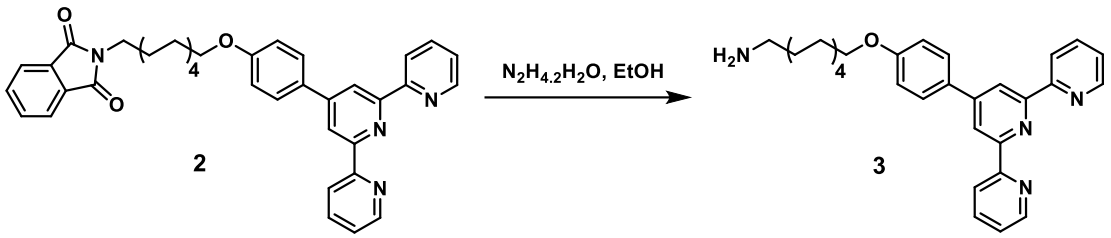

Hydrazine hydrate (450 mg, 8.99 mmol) and compound **2** (1.80 g, 2.95 mmol) were suspended in EtOH (50.0 mL) and heated at reflux for 12 h. After cooling and concentrating *in vacuo*, the residue was partitioned between CH_2Cl_2 and H_2O. The aqueous layer was extracted (3×) with CH_2Cl_2 and the combined organic layer was washed with brine, dried ($MgSO_4$), and then recrystallized from CH_2Cl_2/hexanes (3×) to give **3** as a white solid (1.10 g, 78.0%). Mp: 102.3 – 103.9 °C. ^{1}H NMR (500 MHz, $CDCl_3$) δ 8.73 (d, 2H, *J* = 4.7 Hz), 8.70 (s, 2H), 8.66 (d, 2H, *J* = 7.9 Hz), 7.89 – 7.85 (m, 4H), 7.34 (ddd, 2H, *J* = 7.4, 4.8, 0.8 Hz), 7.01 (d, 2H, *J* = 8.8 Hz), 4.02 (t, 2H, *J* = 6.5 Hz), 2.68 (t, 2H, *J* = 7.0 Hz), 1.84 – 1.79 (m, 2H), 1.57 (s, 2H), 1.50 – 1.43 (m, 4H), 1.38 – 1.31 (m, 10H). ^{13}C NMR (125 MHz, $CDCl_3$) δ 160.2, 156.5, 155.9, 149.9, 149.2, 137.0, 130.6, 128.6, 123.9, 121.5, 118.4, 115.0, 68.3, 42.4, 34.0, 29.7, 29.7, 29.6, 29.5, 29.4, 27.0, 26.2. HRMS (ESI$^+$) Calcd for $C_{31}H_{34}N_4O$ $[M+H]^+$: 481.2967, found: 481.2961, error –1.3 ppm.

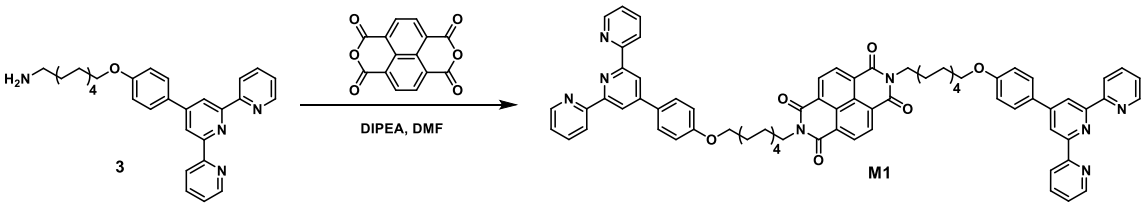

1,4,5,8-Naphthalenetetracarboxylic dianhydride (268 mg, 1.00 mmol) and compound **3** (1.10 g, 2.29 mmol) were dissolved in DMF (80.0 mL). *N*,*N*-Diisopropylethylamine (284 mg, 2.20 mmol) was then added to the reaction mixture, which was then heated to 100 °C and maintained at that temperature for 12 h. The reaction mixture was then cooled to –20 °C to separate out a yellow solid, which was subsequently recrystallized from CH_2Cl_2/hexanes (3×) to give **M1** as a yellow solid (600 mg, 50.3%). Mp: 187.9 – 190.3 °C. ^{1}H NMR (400 MHz, $CDCl_3$) δ 8.72 (d, 4H, *J* = 4.1 Hz), 8.68 (s, 8H), 8.64 (d, 4H, *J* = 8.0 Hz), 7.90 – 7.85 (m, 8H), 7.35 (dd, 4H, *J* = 6.5, 5.1 Hz), 7.01 (d, 4H, *J* = 8.7 Hz), 4.13 (t, 4H, *J* = 7.6 Hz), 4.02 (t, 4H, *J* = 6.4 Hz), 1.85 – 1.78 (m, 4H), 1.74 – 1.68 (m, 4H), 1.50 – 1.35 (m, 24H). ^{13}C NMR (100 MHz, $CDCl_3$) δ 162.9, 160.3, 156.4, 155.8, 149.9, 149.1, 137.1, 131.0, 130.4, 128.6, 126.8, 126.7, 123.9, 121.5, 118.4, 115.0, 68.2, 40.7, 29.5, 29.4, 29.3, 29.3, 29.3, 28.2, 27.2, 26.1. HRMS (ESI$^+$) Calcd for $C_{76}H_{73}N_8O_6$ $[M+H]^+$: 1193.5653, found: 1193.5652, error –0.08 ppm.

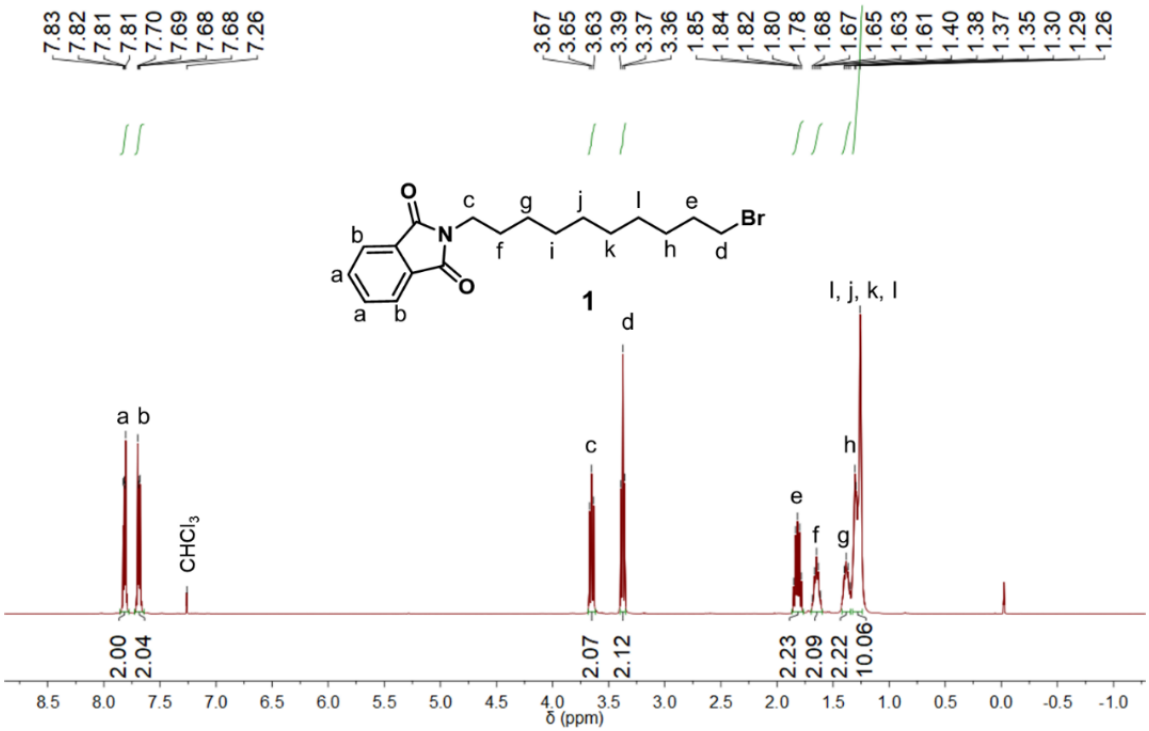

Fig. S2. ^{1}H NMR spectrum ($CDCl_3$, 400 MHz, 298 K) of compound **1**.

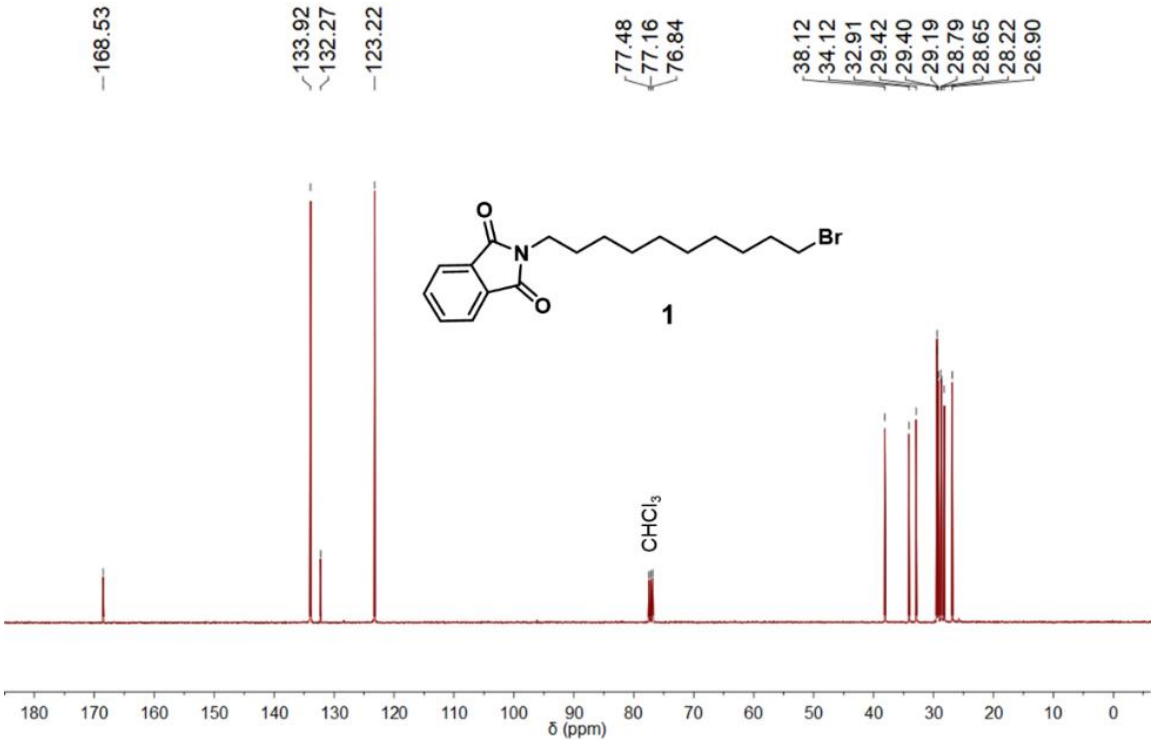

Fig. S3. ^{13}C NMR spectrum ($CDCl_3$, 100 MHz, 298 K) of compound **1**.

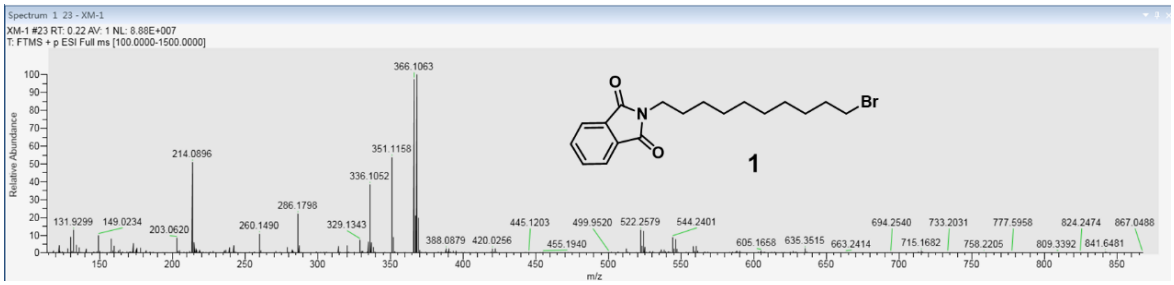

Fig. S4. HR-ESI^{+}-MS spectrum of compound **1**.

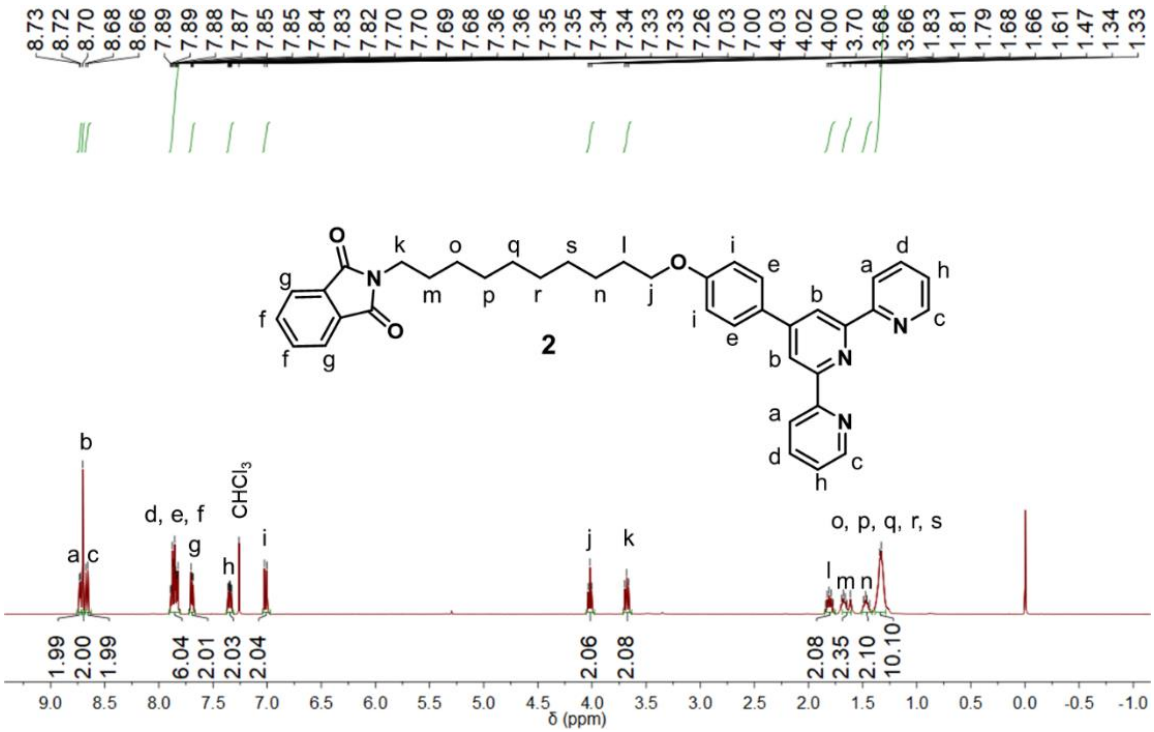

Fig. S5. ^{1}H NMR spectrum ($CDCl_3$, 400 MHz, 298 K) of compound **2**.

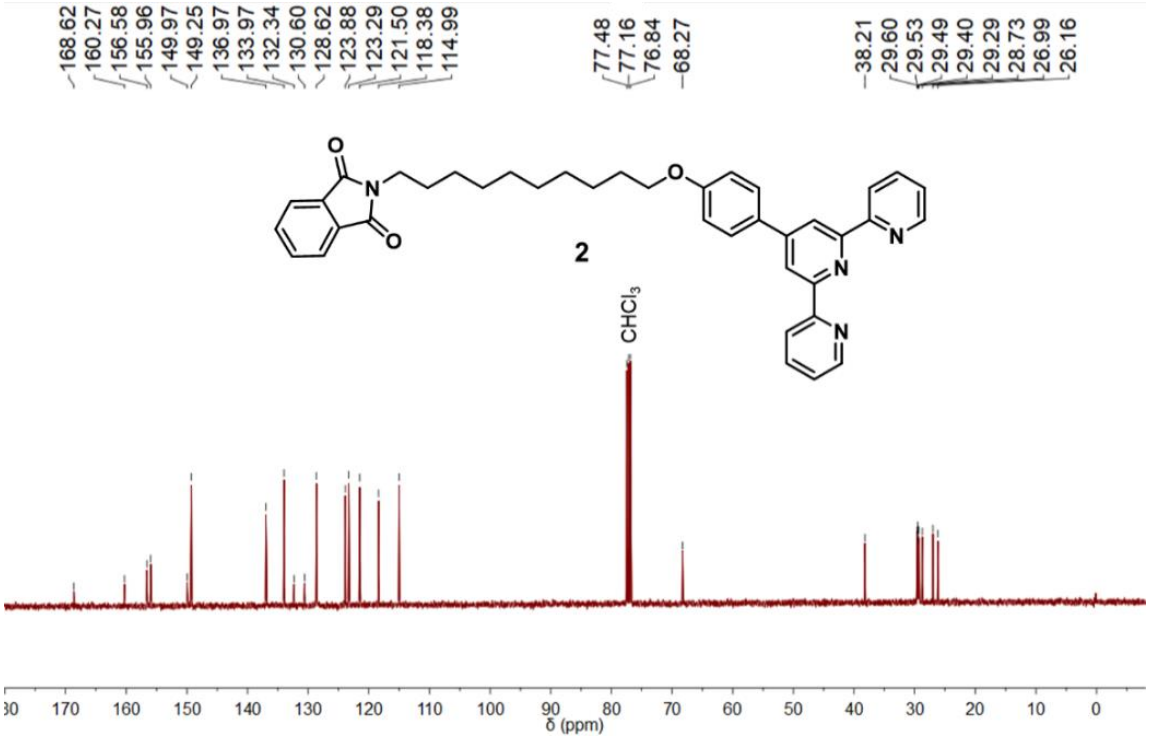

Fig. S6. ^{13}C NMR spectrum ($CDCl_3$, 100 MHz, 298 K) of compound **2**.

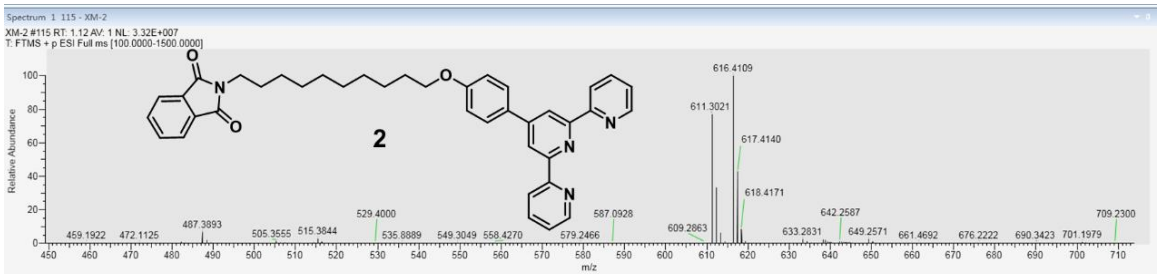

Fig. S7. HR-ESI^{+}-MS spectrum of compound **2**.

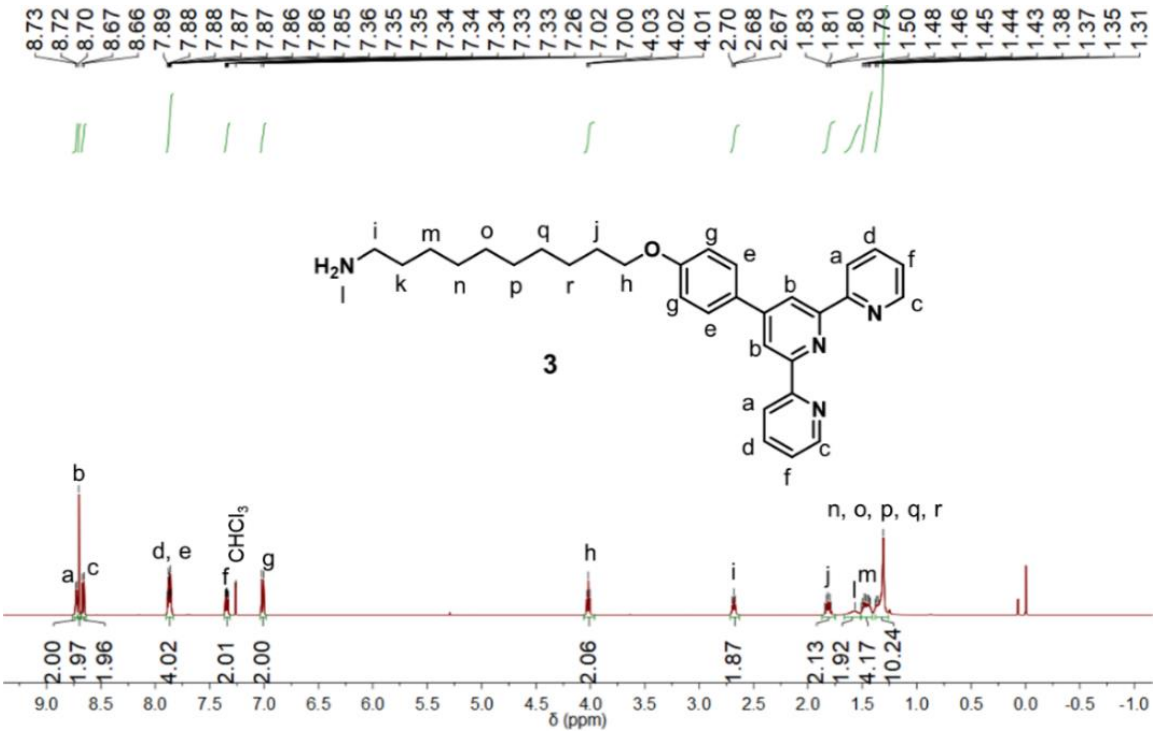

Fig. S8. ^{1}H NMR spectrum ($CDCl_3$, 500 MHz, 298 K) of compound **3**.

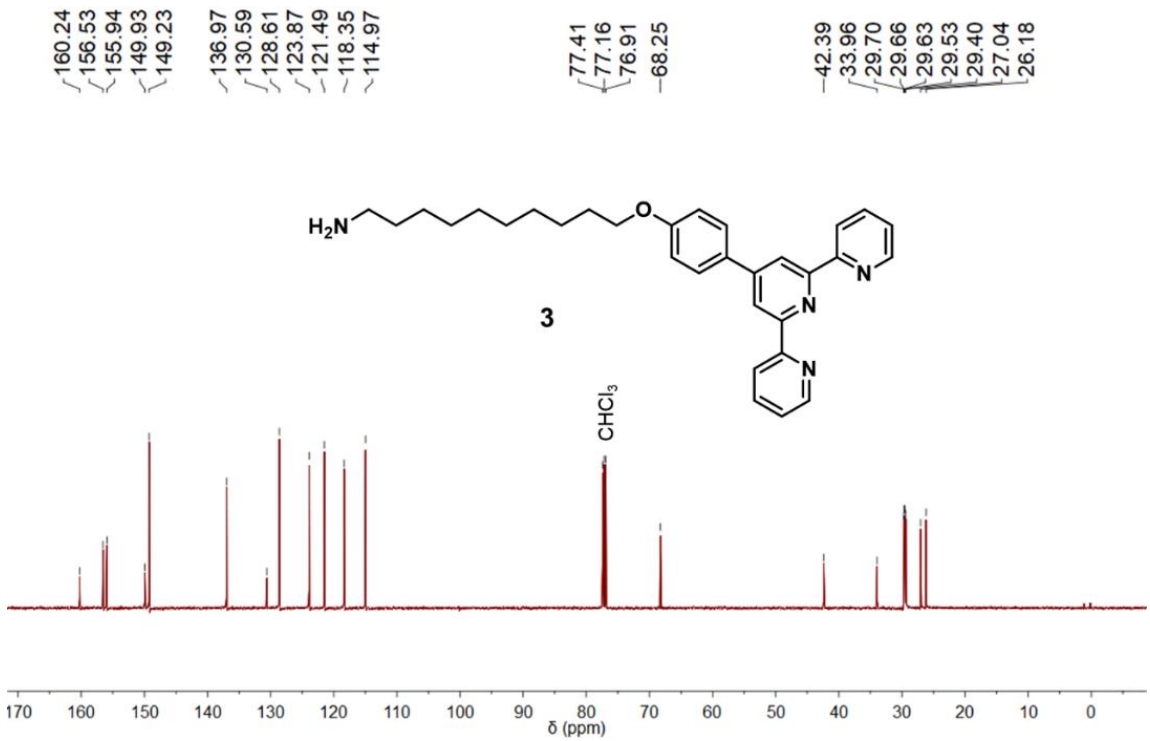

Fig. S9. ^{13}C NMR spectrum ($CDCl_3$, 125 MHz, 298 K) of compound **3**.

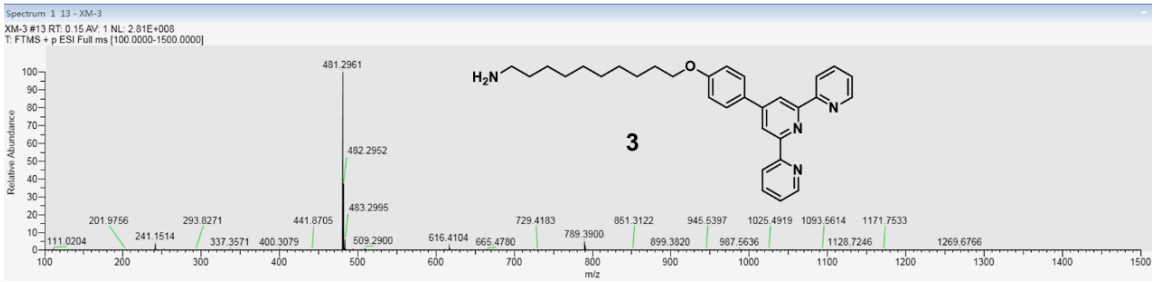

Fig. S10. HR-ESI^{+}-MS spectrum of compound **3**.

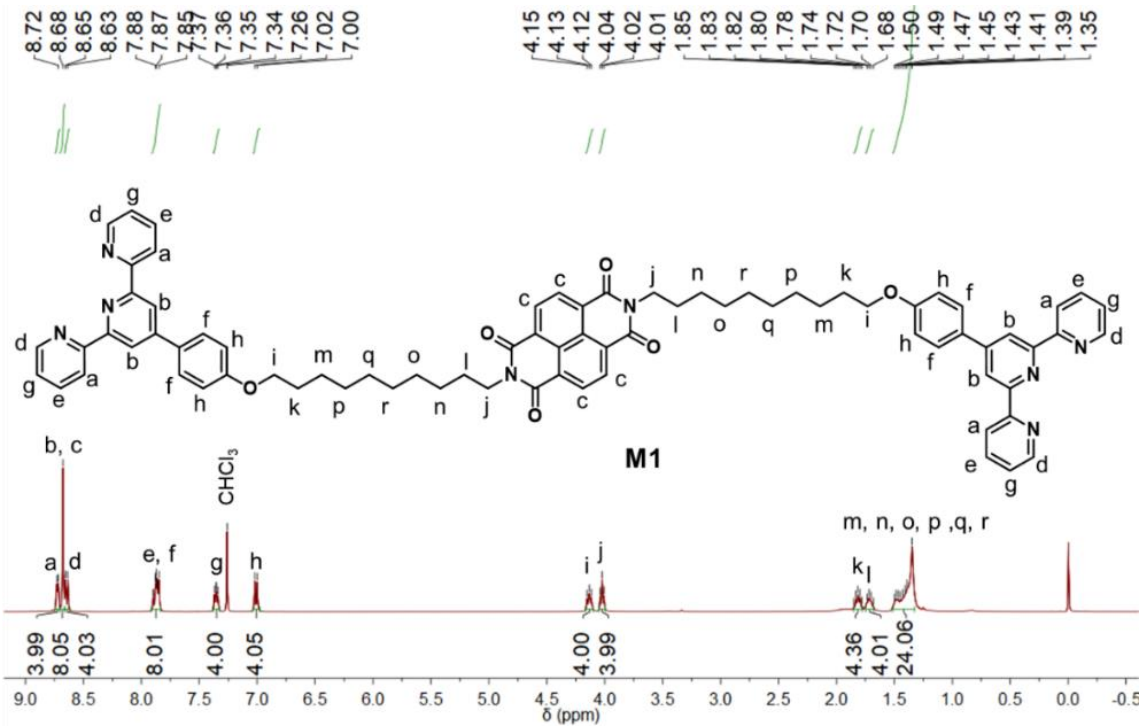

Fig. S11. ^{1}H NMR spectrum ($CDCl_3$, 400 MHz, 298 K) of **M1**.

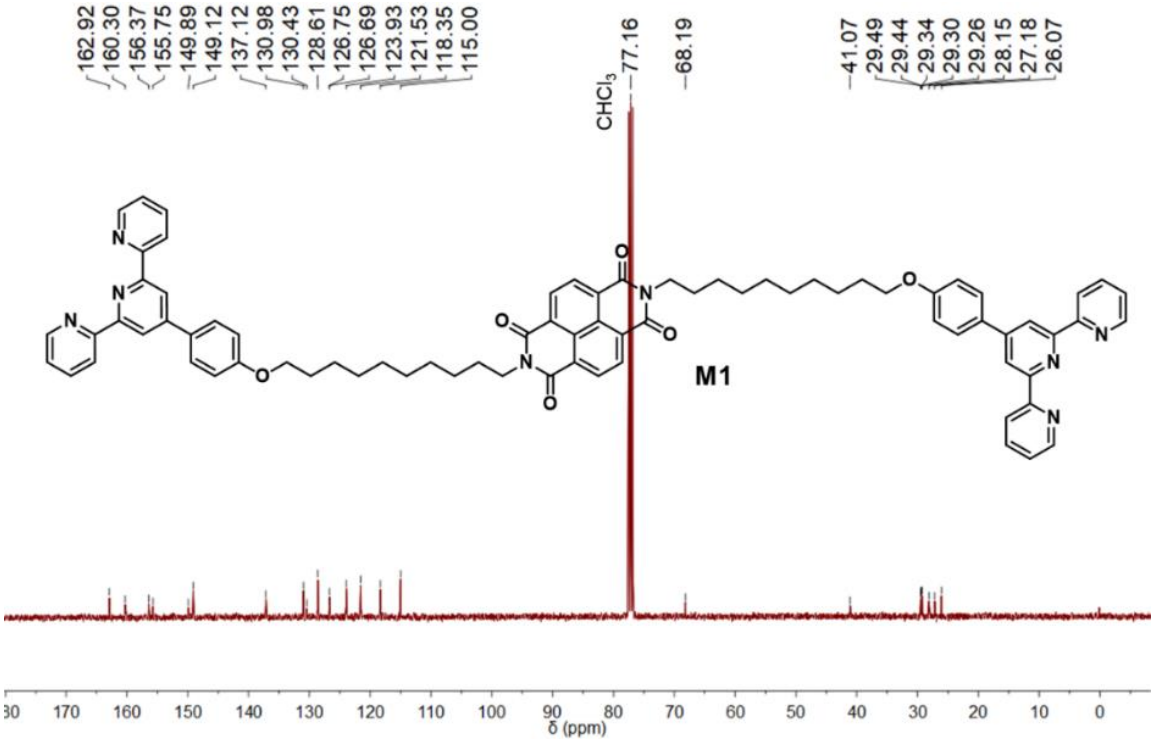

Fig. S12. ^{13}C NMR spectrum ($CDCl_3$, 100 MHz, 298 K) of **M1**.

Acquisition Parameter

Source Type	ESI	Ion Polarity	Positive	Set Nebulizer	0.3 Bar
Focus	Active			Set Dry Heater	180 °C
Scan Begin	50 m/z	Set Capillary	4500 V	Set Dry Gas	4.0 l/min
Scan End	3000 m/z	Set End Plate Offset	-500 V	Set Divert Valve	Waste

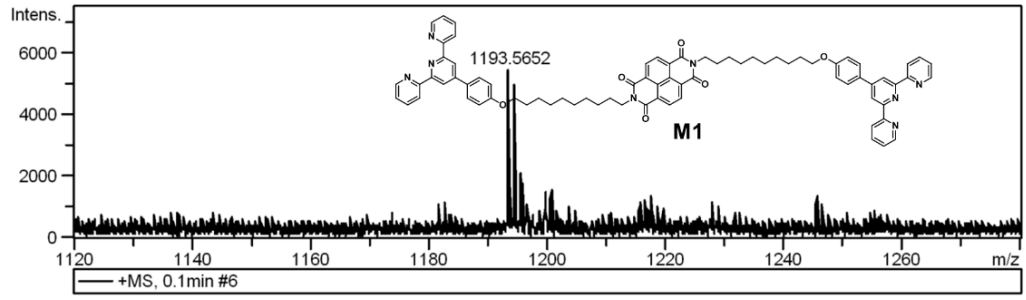

#	m/z	Res.	S/N	I	FWHM
1	1193.5652	11229	18.8	5480	0.1063
2	1194.5668	12141	16.9	4645	0.0984

Fig. S13. HR-ESI^{+}-MS spectrum of **M1**.

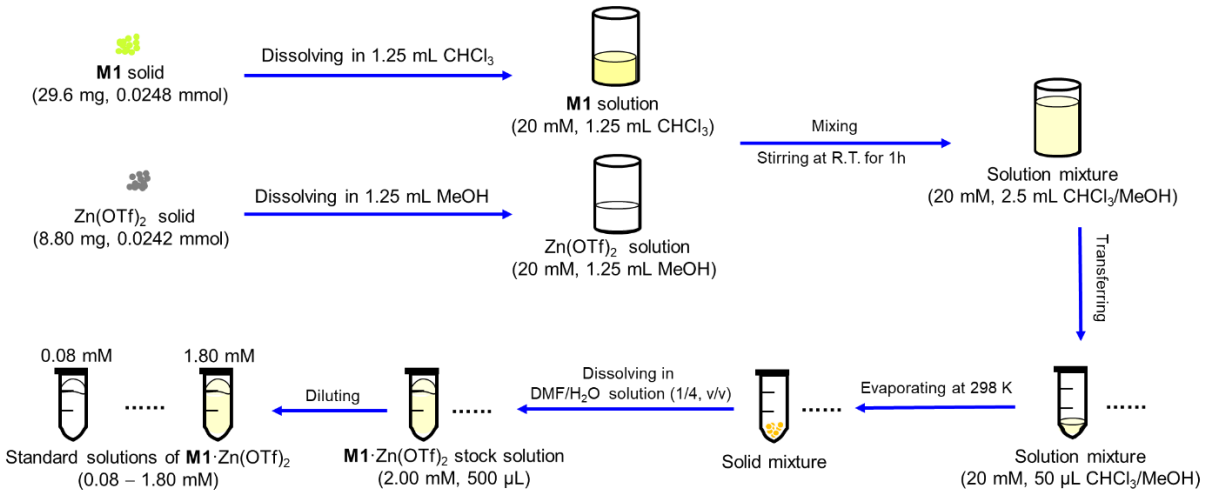

Fig. S14. Flow diagram showing the preparation of various **M1** + $Zn(OTf)_2$ solutions.

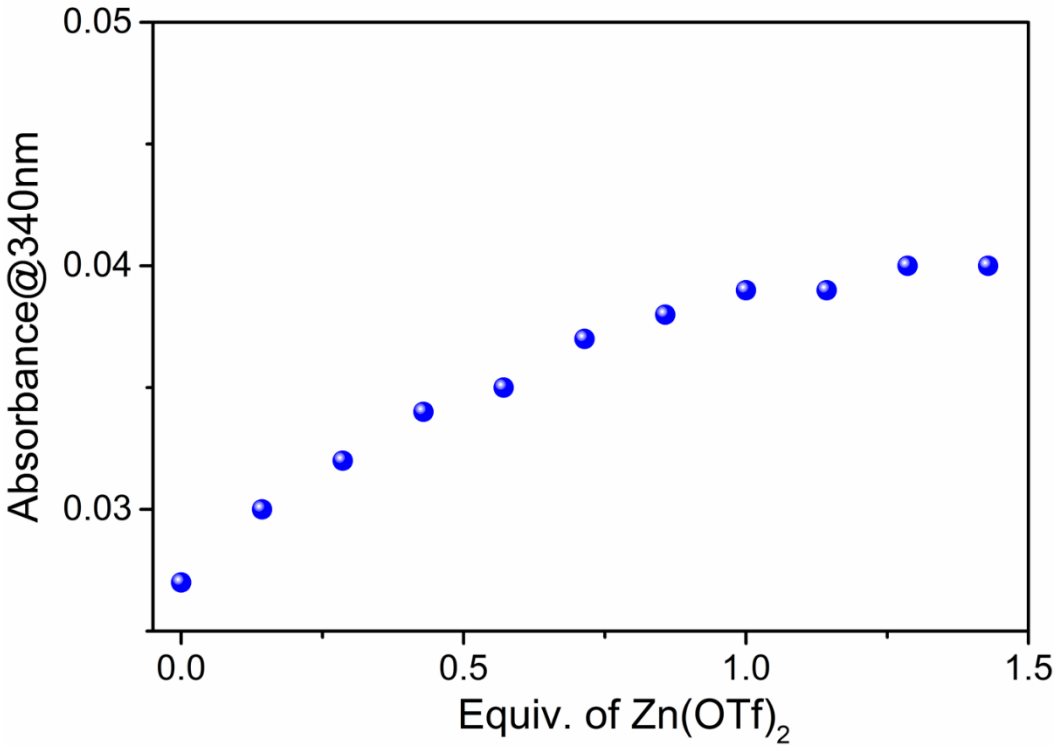

Fig. S15. Plot of the absorbance at 340 nm versus the number of $Zn(OTf)_2$ equivalents.

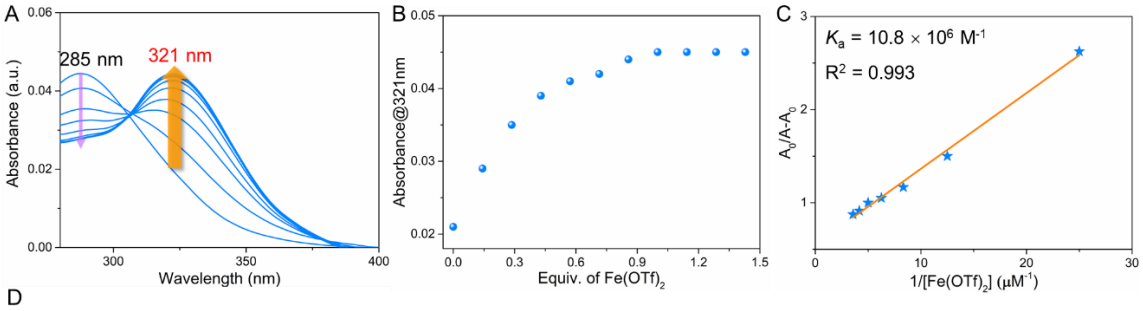

D

[Monomer] (mM)	0.08	0.12	0.16	0.20	0.40	0.60	0.80	1.00	1.20	1.40	1.60	1.80	2.00
DP_{cal}	20.7	25.4	29.3	32.8	46.4	56.8	65.6	73.3	80.3	86.7	92.7	98.4	104

Fig. S16. (*A*) UV-vis spectra of compound **1a** (0.280 μM) in 1.00 mL DMF/H_2O (1/4, v/v) recorded upon the stepwise addition of $Fe(OTf)_2$ (100 μM) at 298 K. (*B*) Plot of the absorbance at 321 nm versus the number of $Fe(OTf)_2$ equivalents. (*C*) Plot of $(A_0/(A-A_0)$ as a function of $1/[Fe(OTf)_2]$. The apparent association constant K_a corresponding to the interaction between **1a** (0.280 μM) and $Fe(OTf)_2$ (100 μM) was determined using the Benesi-Hilderbrand equation $A_0/(A-A_0) = (A_0/(A_{max} - A_0))((1/K_a)\ [Fe(OTf)_2]^{-1} + 1)$. (*D*) The degree of polymerization calculated (DP_{cal}) for equimolar mixtures of **M1** and $Fe(OTf)_2$ (0.08 – 2.00 mM).

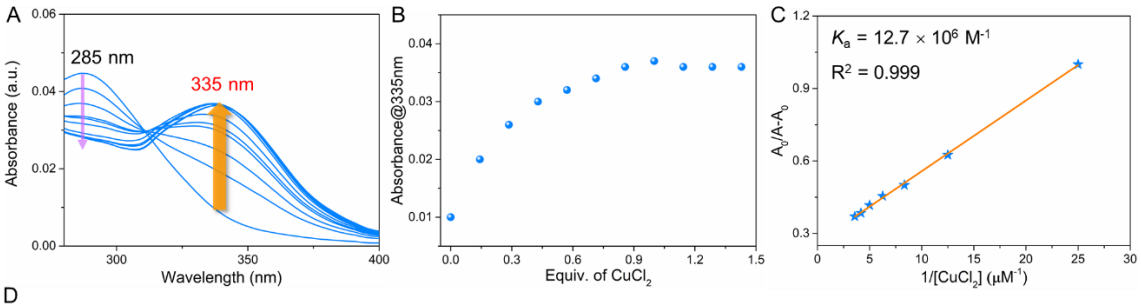

D

[Monomer] (mM)	0.08	0.12	0.16	0.20	0.40	0.60	0.80	1.00	1.20	1.40	1.60	1.80	2.00
DP_{cal}	22.5	27.5	31.8	35.6	50.3	61.6	71.1	79.5	87.1	94.1	101	107	112

Fig. S17. (*A*) UV-vis spectra of compound **1a** (0.280 μM) in 1.00 mL DMF/H_2O (1/4, v/v) recorded upon the stepwise addition of $CuCl_2$ (100 μM) at 298 K. (*B*) Plot of the absorbance at 335 nm versus the number of $CuCl_2$ equivalents. (*C*) Plot of (A_0/(A-A_0) as a function of 1/[$CuCl_2$]. The apparent association constant K_a corresponding to the interaction between **1a** (0.280 μM) and $CuCl_2$ (100 μM) was determined using the Benesi-Hilderbrand equation $A_0/(A-A_0)$ = (A_0/(A_{max} - A_0))((1/K_a) $[CuCl_2]^{-1}$ + 1). (*D*) The degree of polymerization calculated (DP_{cal}) for equimolar mixtures of **M1** and $CuCl_2$ (0.08 – 2.00 mM).

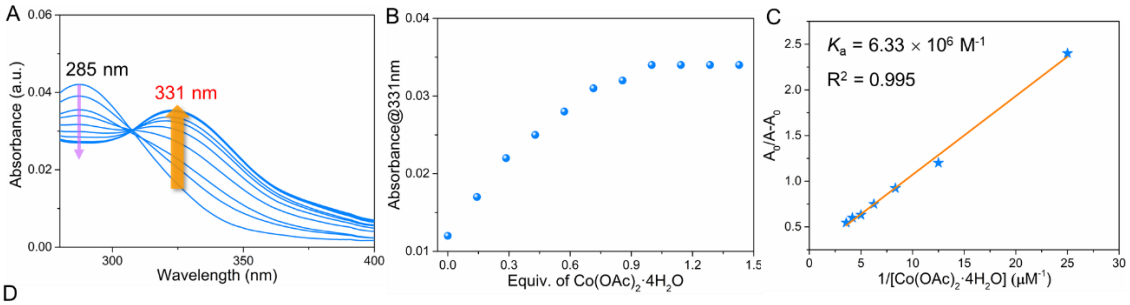

D

[Monomer] (mM)	0.08	0.12	0.16	0.20	0.40	0.60	0.80	1.00	1.20	1.40	1.60	1.80	2.00
DP_{cal}	15.9	19.5	22.5	25.2	35.6	43.6	50.3	56.3	61.6	66.6	71.2	75.5	79.6

Fig. S18. (*A*) UV-vis spectra of compound **1a** (0.280 μM) in 1.00 mL DMF/H_2O (1/4, v/v) recorded upon the stepwise addition of $Co(OAc)_2{\cdot}4H_2O$ (100 μM) at 298 K. (*B*) Plot of the absorbance at 331 nm versus the number of $Co(OAc)_2{\cdot}4H_2O$ equivalents. (*C*) Plot of (A_0/(A-A_0) as a function of 1/[$Co(OAc)_2{\cdot}4H_2O$]. The apparent association constant K_a corresponding to the interaction between **1a** (0.280 μM) and $Co(OAc)_2{\cdot}4H_2O$ (100 μM) was determined using the Benesi-Hilderbrand equation $A_0/(A-A_0) = (A_0/(A_{max} - A_0))((1/K_a)\ [Co(OAc)_2{\cdot}4H_2O]^{-1} + 1)$. (*D*) The degree of polymerization calculated (DP_{cal}) for equimolar mixtures of **M1** and $Co(OAc)_2{\cdot}4H_2O$ (0.08 – 2.00 mM).

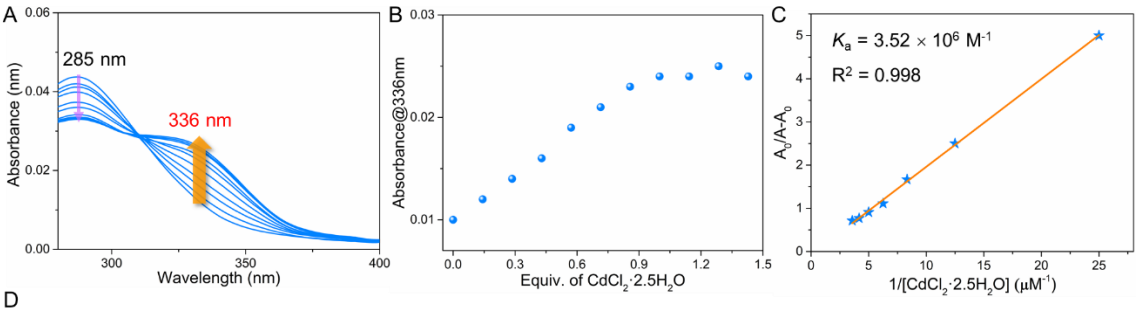

D

[Monomer] (mM)	0.08	0.12	0.16	0.20	0.40	0.60	0.80	1.00	1.20	1.40	1.60	1.80	2.00
DP_{cal}	11.9	14.5	16.8	18.7	26.5	32.5	37.5	41.9	45.9	49.6	53.0	56.2	59.3

Fig. S19. (*A*) UV-vis spectra of compound **1a** (0.280 μM) in 1.00 mL DMF/H_2O (1/4, v/v) recorded upon the stepwise addition of $CdCl_2·2.5H_2O$ (100 μM) at 298 K. (*B*) Plot of the absorbance at 336 nm versus the number of $CdCl_2·2.5H_2O$ equivalents. (*C*) Plot of (A_0/(A-A_0) as a function of 1/[$CdCl_2·2.5H_2O$]. The apparent association constant K_a corresponding to the interaction between **1a** (0.280 μM) and $CdCl_2·2.5H_2O$ (100 μM) was determined using the Benesi-Hilderbrand equation $A_0/(A-A_0) = (A_0/(A_{max} - A_0))((1/K_a)\ [CdCl_2·2.5H_2O]^{-1} + 1)$. (*D*) The degree of polymerization calculated (DP_{cal}) for equimolar mixtures of **M1** and $CdCl_2·2.5H_2O$ (0.08 – 2.00 mM).

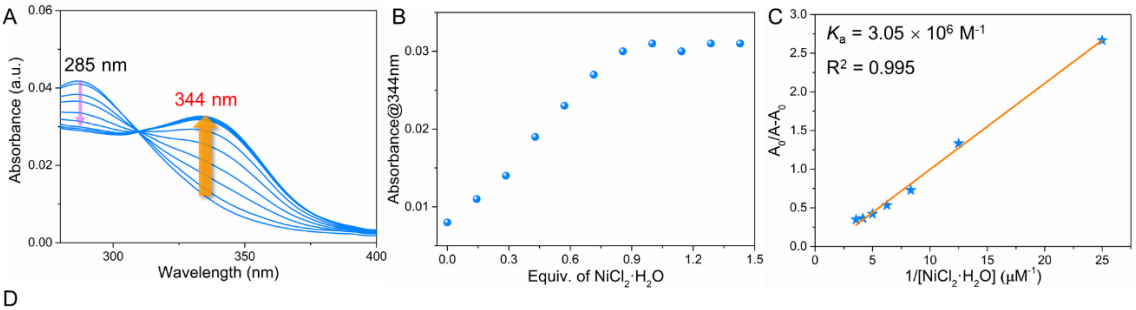

D

[Monomer] (mM)	0.08	0.12	0.16	0.20	0.40	0.60	0.80	1.00	1.20	1.40	1.60	1.80	2.00
DP_{cal}	11.0	13.5	15.6	17.5	24.7	30.3	34.9	39.1	42.8	46.2	49.4	52.4	55.2

Fig. S20. (*A*) UV-vis spectra of compound **1a** (0.280 μM) in 1.00 mL DMF/H_2O (1/4, v/v) recorded upon the stepwise addition of $NiCl_2{\cdot}H_2O$ (100 μM) at 298 K. (*B*) Plot of the absorbance at 344 nm versus the number of $NiCl_2{\cdot}H_2O$ equivalents. (*C*) Plot of (A_0/(A-A_0) as a function of 1/[$NiCl_2{\cdot}H_2O$]. The apparent association constant K_a corresponding to the interaction between **1a** (0.280 μM) and $NiCl_2{\cdot}H_2O$ (100 μM) was determined using the Benesi-Hilderbrand equation $A_0/(A\text{-}A_0) = (A_0/(A_{max} - A_0))((1/K_a)\ [NiCl_2{\cdot}H_2O]^{-1} + 1)$. (*D*) The degree of polymerization calculated (DP_{cal}) for equimolar mixtures of **M1** and $NiCl_2{\cdot}H_2O$ (0.08 – 2.00 mM).

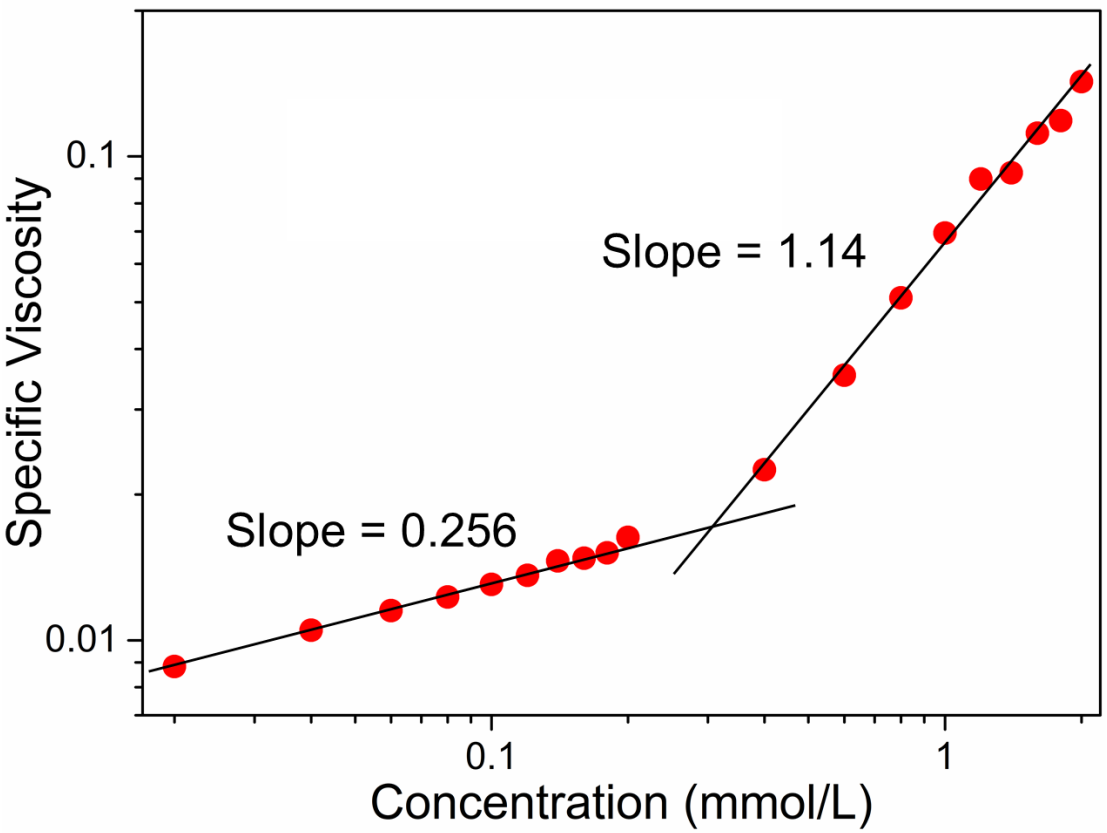

Fig. S21. Plot of the specific viscosity of equimolar mixtures of **M1** + $Zn(OTf)_2$ in DMF/H_2O (1/4, v/v) versus their concentration at 298 K.

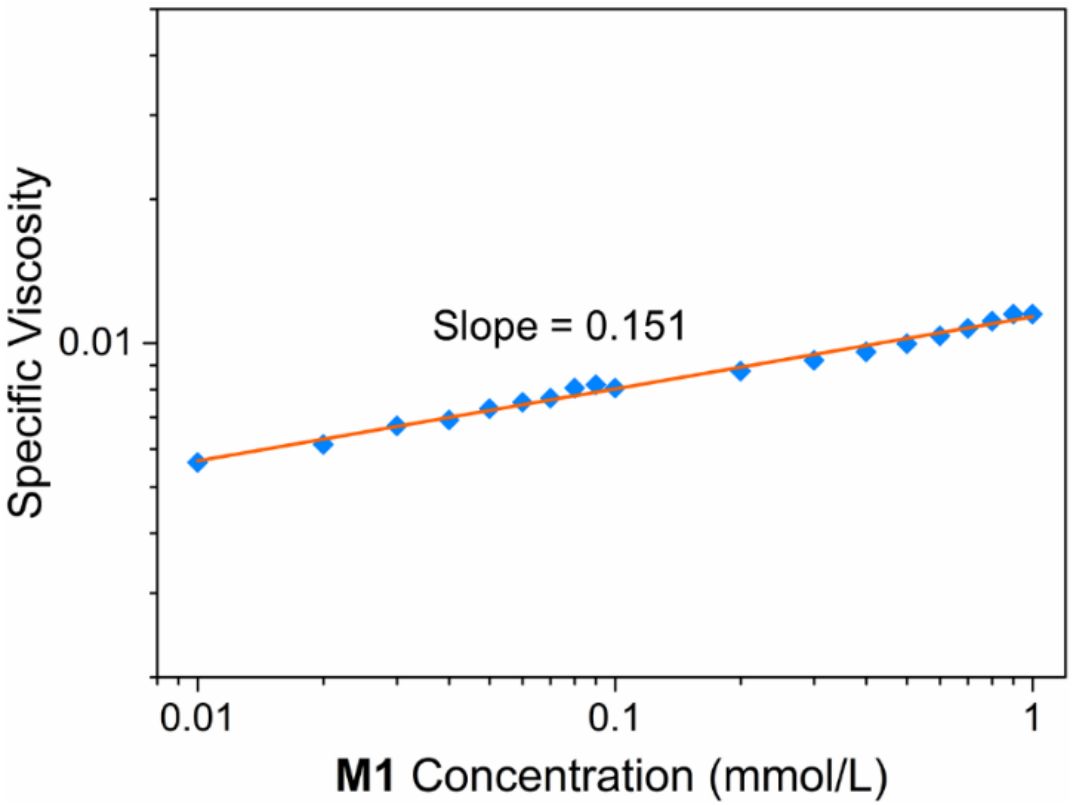

Fig. S22. Log-log plot of the specific viscosity of **M1** solutions (DMF/H_2O = 1/4, v/v) (298 K) versus the monomer concentration.

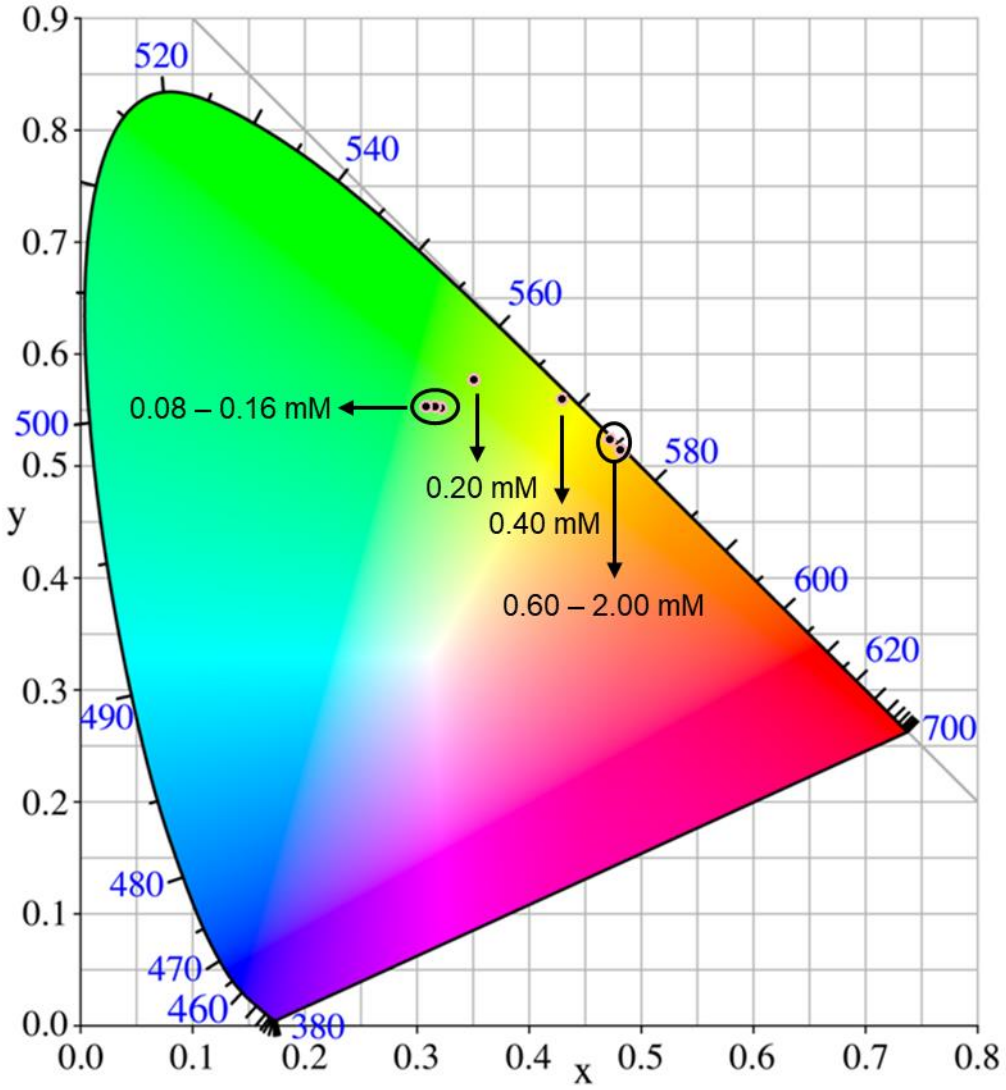

Fig. S23. Commission Internationale de l'Eclairage (CIE) 1931 chromaticity diagram for equimolar mixtures of **M1** and $Zn(OTf)_2$ monitored at different total concentrations (0.08, 0.12, 0.16, 0.20, 0.40, 0.80, 1.20, 1.40, 1.60, 1.80, 2.00 mM in DMF/H_2O (1/4, v/v)).

Movie S1 (separate file). Related to Fig. 4*D*. Dilution of an equimolar solution of **M1** + $Zn(OTf)_2$ monitored under UV light (365 nm; handheld UV lamp).

Movie S2 (separate file). Related to Fig. 7*D*. Dilution of a solution of **M1** monitored under UV light (365 nm; handheld UV lamp).

SI References

1. M. Wang, *et al*., Design and synthesis of self-included pillar[5]arene-based bis-[1]rotaxanes. *Chin. Chem. Lett.* **30**, 345-348 (2019).
2. Y.-T. Chan, C. N. Moorefield, G. R. Newkome, Synthesis, characterization, and self-assembled nanofibers of carbohydrate-functionalized mono- and di(2,2′:6′,2″-terpyridinyl)arenes. *Chem. Commun.* 6928-6930 (2009).
3. Z. M. Hudson, D. J. Lunn, M. A. Winnik, I. Manners, Colour-tunable fluorescent multiblock micelles. *Nat. Commun.* **5**, 3372 (2014).